arXiv:cond-mat/0502093v1 [cond-mat.str-el] 3 Feb 2005

Charge-induced maximal spin states of a polynuclear transition-metal complex

C. Romeike[1], M. R. Wegewijs[1], M. Ruben[2], W. Wenzel[2], and H. Schoeller[1]
[1] *Institut für Theoretische Physik A, RWTH Aachen, 52056 Aachen, Germany*
[2] *Institut für Nanotechnologie, Forschungszentrum Karlsruhe, 76021 Karlsruhe, Germany*
(Dated: February 2, 2008)

We theoretically investigate the ground state spin of a polynuclear transition-metal complex as a function of the number of added electrons taking into account strong electron correlations. Our phenomenological model of the so-called $[2 \times 2]$-grid molecule incorporates the relevant electronic degrees of freedom on the four transition-metal centers (either Fe^{2+} or Co^{2+}) and the four organic bridging ligands. Extra electrons preferably occupy redox orbitals on the ligands. Magnetic interactions between these ligands are mediated by transition-metal ions *and vice versa*. Using both perturbation theory and exact diagonalization we find that for certain charge states the maximally attainable total spin (either $S_{\text{tot}} = 3/2$ or $S_{\text{tot}} = 7/2$) may actually be achieved. Due to the Nagaoka mechanism, all unpaired electron spins couple to a total maximal spin, including unpaired electron spins on the metal-ions in the case of Co^{2+}. The parameters are chosen to be consistent with cyclovoltammetry experiments in which up to twelve redox states have been observed. The above effect may also be realized in other complexes with an appropriate connectivity between the redox sites. The maximal spin states of such a charge-switchable molecular magnet may be experimentally observed as spin-blockade effects on the electron tunneling in a three-terminal transport setup.

PACS numbers:

I. INTRODUCTION

The synthesis and investigation of molecule based magnets have been active areas of research for almost a decade [1, 2]. Today molecule based magnets offer a variety of chemical and magnetic properties which have potential applications in a wide range of systems. Photo-magnetic (e.g. $K_{0.4}Co_{1.3}[Fe(CN)_6]$) or spin-crossover magnetic substances (e.g. Fe(o-phenanthroline)$_2$(NCS)$_2$) offer potential applications in switchable devices. Polynuclear transition-metal complexes are particularly attractive in the effort to design molecules with magnetic centers which couple either ferro- or antiferromagnetically. Interesting quantum tunneling effects were reported for ferromagnetic molecules, e.g. Mn_{12} [3] and Fe_8 [4]. Antiferromagnets are of interest also due to effects associated with the Néel-vector [5, 6, 7]. One interesting class of highly-designable complexes is the $[M \times M]$-grid structure which is formed by self-assembly [8, 9, 10, 11]. It consists of M^2 transition-metal centers which are positioned by two perpendicular arrays of rod-like ligands, each with M coordination sites. The transition-metals typically lie in a plane due to symmetric positioning of the ligands. Several realizations of these supramolecules exist which exhibit a variety of magnetic and electrochemical properties, which can be manipulated via sidegroup substitutions. In this paper we focus in particular on the $[2\times2]$-grid depicted in Figure 1. It consists of four organic ligands (bis(bipyridyl)-bipyrimidine) and four transition-metal ions (e.g. Mn^{2+}, Fe^{2+}, Co^{2+}, Ni^{2+} or Zn^{2+} [12]). Each metal-ion is situated in an approximately octahedral environment of nitrogen atoms. The total charge 8+ of the complex is countered by anions, e.g. BF_4^-. The Co^{2+}-$[2 \times 2]$-grid exhibits an impressive twelve reversible

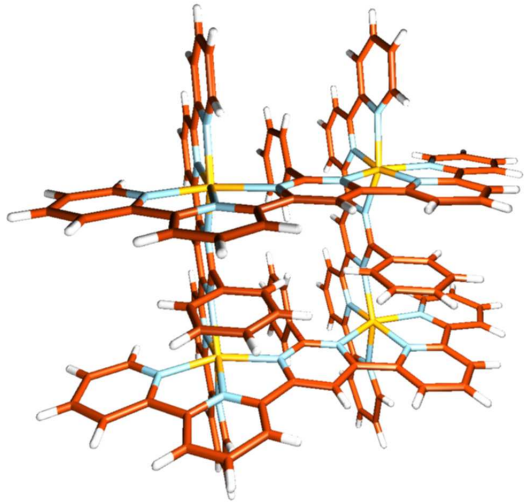

FIG. 1: Structure of the $[2 \times 2]$-grid-type complex.

reduction steps in solution in a cyclic voltammetry at $T = 253K$ [12]. It is also possible to trap and identify these complexes on a graphite surface in a controlled way [13]. Furthermore, in Co^{2+}-$[2 \times 2]$-grids the spin of each metal-ion was found to be $S = 1/2$ at low temperature and their intramolecular magnetic coupling was demonstrated to be antiferromagnetic [14].

We have developed a phenomenological strongly-correlated electron model which represents the important spin and charge degrees of freedom that play a role in both the redox chemistry and the magnetic interactions of $[2 \times 2]$-grid complexes. We include the strong electrostatic interactions between electrons localized on the metal-ions and the ligands as well as the weak tunnel-

ing of electrons between them. A crucial feature of our model is that the orbital and charging energies on the ligands and ions are very different, a situation common in transition-metal complexes. We are interested in how the electron spins on the molecule couple to form the total magnetic moment and how this coupling is affected by total electron number which can be electrically controlled in a three terminal transport setup (which is not considered here). The metal-ions mediate the coupling between electrons on the ligands *and vice versa*. We also want to study the effect of an unpaired electron spin on a mediating metal-ion on the ligand-ligand spin coupling, which will in turn determine the total spin formed by the ion and ligand subsystems. Two simple cases are therefore considered, assuming each ion is in a low-spin state: either $S = 0$, Fe^{2+}, or $S = 1/2$, Co^{2+}. The Coulomb interaction also generates direct exchange coupling between unpaired electrons on ligands and metal-ions which we also take into account. We focus on how the spins couple to a magnetic moment of large magnitude due to strong Coulomb and kinetic effects depending on the total charge. We do not consider effects on smaller energy scales which determine the preferred direction of the magnetic moment.

As expected, an antiferromagnetic coupling between the metal-ion and ligand subsystems prevails for most total charge numbers. Extra electrons added to the bridging ligands introduce a ferromagnetic spin correlation between the metal-ions if the latter have a spin. However, we find that near half-filling of the four ligand orbitals sufficiently strong Coulomb interactions can stabilize a *maximal spin ground state* ($S_{\mathsf{tot}} = 3/2$ for Fe^{2+} and $7/2$ for Co^{2+}) by the Nagaoka mechanism [15]. Due to the Pauli principle a missing or excess electron on the ligands (relative to half-filling) can be delocalized maximally when the "background" of the remaining electrons is completely spin-polarized. In our model this effect is most easily achieved for a Fe^{2+}-$[2 \times 2]$- grid. For a Co^{2+}-$[2 \times 2]$-grid the spins of electrons localized on the bridging metal-ions counteract the Nagaoka mechanism. However, the direct exchange coupling between unpaired electrons on the neighboring ligands and metal-ions cooperates with the Nagaoka mechanism [16]. The resulting maximal spin is however more than twice as large as for Fe^{2+}. The charge-sensitive spin-polarization requires a strong local Coulomb charging effect and metal-to-ligand charge-transfer (MLCT) barrier. The former can be achieved chemically by introducing electron-donating sidegroups on the ligands [12]. The electrochemical experiments [12] were performed near room temperature where thermal occupation of high-spin excited states of the metal-ions becomes possible. Generalization of our model to incorporate the high-spin states of the ions is, however, nontrivial since vibrational degrees of freedom of the nuclear framework are involved in their stabilization [17]. This is beyond the scope of the present paper where we focus on low temperature behavior.

Experimental detection of sublattice and total magnetization as a function of the number of added electrons would be of great interest. In particular, we propose electron transport through the complex in a three terminal setup. In a gate voltage range where the ligand orbitals are near half-filling the large change in ground state spin $\big(\Delta S_{\mathsf{tot}} = 3/2$ (Fe^{2+}), resp. $\Delta S_{\mathsf{tot}} = 7/2$ (Co^{2+}) $\big)$ may be revealed through the *spin-blockade* effect [18]. We have investigated this transport problem in detail for a simple generic model n [19]. The goal of the present paper is to derive and investigate the effective model, in particular the effect of bridging metal-ions with a spin. Experiments in semiconductor heterostructures show that a transport current can couple through the spin-blockade effect to electron spins localized in a quantum dot and subsequently to nuclear spins in the local environment via the hyperfine interaction [20]. This offers an interesting perspective for single-molecule transport where the immediate nuclear environment of the device can be controlled at the level of chemical synthesis.

The paper is organized as follows. In section II we discuss the minimal set of orbitals involved in electron addition processes and the intramolecular magnetic coupling. This serves as a motivation for the correlated electron model which we introduce in section III. In section IV we discuss a perturbative treatment of the ion-ligand tunneling in this model to gain a simple understanding of the role of spin degrees of freedom on the ions. We obtain the ground states and low energy total-spin excitations in sections V A and V B. We discuss the electron addition energies and the modulation of the ground state spin as a function of the number of added electrons. We conclude with a discussion of implications for electron tunneling experiments in section VI.

II. ELECTRONIC STRUCTURE

We can expect that the dominant molecular orbitals (MOs) at the Fermi energy are either d-like orbitals from the metal 2+ ions or π-orbitals from the ligands. The electrochemical experiments [12] indicated that additional electrons occupy orbitals localized mostly on the *ligands*, which is not uncommon for polypyridine complexes [21].

Let us first consider the individual metal-ions which are coordinated by six nitrogen atoms. In a ligand-field picture, an octahedral coordination of each metal-ion in the grid would cause their d-orbitals to split up into two shells, t_{2g} (d_{xy}, d_{xz}, d_{yz}) and e_g ($d_{x^2-y^2}, d_{z^2}$). However, the symmetry of the local environment is lower and results in a small splitting of the levels in each shell. The different orbital occupations for Fe^{2+} and Co^{2+} are shown in Figure 2. In the case of Fe^{2+} in its low-spin configuration the t_{2g} shell is closed and the e_g orbitals are empty. In the case of Co^{2+} there is an additional unpaired electron in the lowest of the two e_g orbitals.

The highest occupied molecular orbitals of the ligands are mostly of π character as ab-initio calculations show.

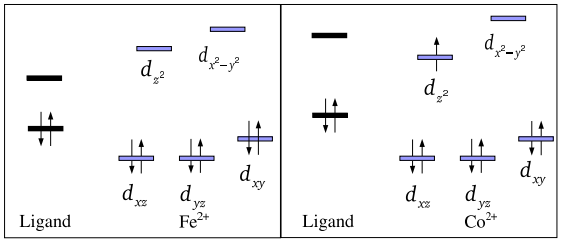

FIG. 2: Orbital configuration of transition metal-ions and ligands.

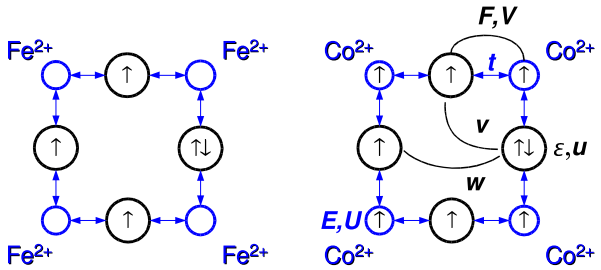

FIG. 3: Geometry of transition-metal $[2\times 2]$-grid consisting of metal-ion orbitals (small circles), Fe^{2+} (left) and Co^{2+} (right), connected by ligands (large circles). The hopping t, orbital energies E, ϵ and Coulomb charging U, V, u, v, w and direct exchange energy F are shown schematically.

The important point is that the empty or singly occupied e_g-orbitals on the metal-ions have different approximate symmetry (σ). This means we can consider ligands and metal-ions weakly coupled systems and discuss the tunneling of electrons between them. The remaining question is whether extra electrons prefer to occupy the metal-ion d-orbitals or the ligand π-orbitals. As far as charging effects are concerned, one expects that the on-site energy U on the metal ions is larger than the on-site energy u on the ligands because orbitals are more contracted on the metal-ions. Furthermore, electrons would favor positions between two positively charged ions, i.e. on the bridging ligand. This is in line with the interpretation of the cyclovoltammetry experiments [12]. The main difference in our model between the Co^{2+}/Fe^{2+}-$[2\times 2]$-grids will thus be the presence/absence of an localized, unpaired electron in an orbital of the metal-ion bridging the two ligands (Figures 2, 3).

III. CHARGING MODEL

We model the $[2\times 2]$-grid complex by four metal (Fe^{2+} or Co^{2+}) and four ligand sites with one spin-degenerate orbital per site (Figure 3). The following Hamiltonian then captures the features of the electronic degrees of freedom discussed in section II:

$$
\begin{aligned}
H &= H_{\mathsf{T}} + H_{\mathsf{L}} + H_{\mathsf{Fe/Co}} + H_{\mathsf{dir}} + H_{\mathsf{V}}, && (1)\\
H_{\mathsf{T}} &= \sum_{\langle i,j\rangle}\sum_{\sigma} t\, A^{\dagger}_{i,\sigma} a_{j,\sigma} + h.c. && (2)\\
H_{\mathsf{L}} &= \sum_{j=1}^{4}(\epsilon n_j + u\, n_{j,\uparrow} n_{j,\downarrow} + v\, n_j n_{j+1})\\
&+ w\sum_{j=1}^{2} n_j n_{j+2} && (3)\\
H_{\mathsf{Fe/Co}} &= \sum_{i=1}^{4}(E N_i + U\, N_{i,\uparrow} N_{i,\downarrow}) && (4)\\
H_{\mathsf{dir}} &= F\sum_{\sigma,\sigma'}\sum_{\langle i,j\rangle} A^{\dagger}_{i,\sigma} a^{\dagger}_{j,\sigma'} A_{i,\sigma'} a_{j,\sigma}\\
&= -2F\sum_{\langle i,j\rangle}(\mathbf{S}_i \mathbf{s}_{j,j} + \frac{1}{4} N_i\, n_j) && (5)\\
H_{\mathsf{V}} &= V\sum_{\langle i,j\rangle} N_i\, n_j. && (6)
\end{aligned}
$$

Operators and variables (except t, F, V) in lower/upper case relate to the metal-ion/ligands and it is implicitly understood that all indices appearing run from 1 to 4 (e.g. $j+1\to 1$ for $j=4$). $\langle i,j\rangle$ denotes a summation over nearest neighbor metal-ions ($i=1-4$) and ligands ($j=1-4$). The Fermion operator $a^{\dagger}_{j,\sigma}$ ($a_{j,\sigma}$) creates (destroys) an electron on ligand site $j=1-4$ with spin projection $\sigma=\pm 1/2$. The occupation number operator is defined as usual $n_{j,\sigma}=a^{\dagger}_{j,\sigma}a_{j,\sigma}$ and $n_j=\sum_\sigma n_{j,\sigma}$. Similar definitions hold for the metal-ion ($A_{i,\sigma}, N_{i,\sigma} = A^{\dagger}_{i,\sigma}A_{i,\sigma}, N_i=\sum_\sigma N_{i,\sigma}$). $\boldsymbol{S}_i = \frac{1}{2}\sum_{\sigma,\sigma'} A^{\dagger}_{i,\sigma}\boldsymbol{\tau}_{\sigma,\sigma'}A_{i,\sigma'}$, where $\boldsymbol{\tau}$ is the vector of Pauli matrices, is the electron spin of a metal-ion and $\mathbf{s}_{j,k}=\frac{1}{2}\sum_{\sigma,\sigma'} a^{\dagger}_{j,\sigma}\boldsymbol{\tau}_{\sigma,\sigma'}a_{k,\sigma'}$, is an operator related to the ligands. The tunneling term (2) describes hopping between ligand and metal-ions. For a D_{2d} symmetric molecular structure the hopping matrix elements t are independent of sites. In the following we choose $t=1$ and all energies are expressed in units of t. The ligand-part of the Hamiltonian in (3) consists of a spin independent orbital energy ϵ, the classical Coulomb repulsion terms on the ligand (u) and between adjacent (v) and the opposite ligands (w). Due to decreasing overlap with distance we have $u > v/2 \geq w$ (e.g. for Fe^{2+} $u\approx 4v\approx 0.3eV$ and $v\approx 2w$ [12]). Equation (4) describes the isolated metal-ion orbitals with energy E. For the metal-ions we only consider the short-range interaction U because the orbital overlap between two ions is much smaller than that between two ligands. In order to describe the spin coupling of metal-ion and ligand electrons correctly, we include the direct exchange (5) with $F>0$, which is known to stabilize ferromagnetic states even when it is *weak* [16] (see sections IV and V). For consistency the metal-ligand charging energy (6) also needs to be incorporated. In general $F \lesssim V$ are of the

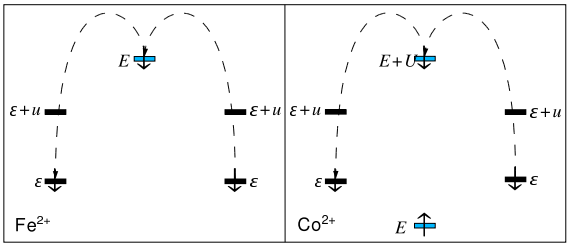

FIG. 4: Energy diagram: Example of a charge transfer from one ligand to another ligand by virtual occupation of Fe^{2+}/Co^{2+}-ion state in the middle. Note that the MLCT barrier $\Delta = \epsilon - E$ is negative in the case of Fe^{2+} and positive in the case of Co^{2+}. Also, for Fe^{2+} the doubly occupied state with energy $E+U$ can be neglected in the perturbation theory.

same order. However, in the regime of interest the particle number on the metal-ions is fixed ($N = 0$ for Fe^{2+}, $N = 4$ for Co^{2+}, cf. section II), so the second term in (5,6) yield a constant. In Figure 3 these interactions are schematically indicated.

We study the parameter regime where the first eight extra electrons will occupy the ligands as in the experiment [12]. (To describe more than 8 reduction steps more than one orbital per ligand has to be taken into account. This is not our purpose here.) For Fe^{2+} we must then assume that the two charge states of the ligand lie below the Fe^{2+} orbital energy E:

$$Fe^{2+} : \epsilon < \epsilon + u < E < E + U \tag{7}$$

For Co^{2+} the two charge states of the ligand lie *between* the singly and doubly occupied states of the metal-ion:

$$Co^{2+} : E < \epsilon < \epsilon + u < E + U \tag{8}$$

The orbital energy difference $\Delta = \epsilon - E$ is associated with metal-ion to ligand charge transfer (MLCT) between unoccupied metal-ion and ligand sites. In the case of Fe^{2+} $\Delta < 0$ and in the case of Co^{2+} $\Delta > 0$.

IV. PERTURBATION THEORY - EFFECTIVE MODEL

In the limit $|\Delta| \gg |t|$ (Fe^{2+}), resp. $\Delta, U - \Delta \gg |t|$ (Co^{2+}) the charge transfer between ligands and metal-ions is suppressed. In order to gain qualitative insight the fluctuations of the orbital occupation around zero (Fe^{2+}) or one (Co^{2+}) can be treated using 2nd order Brillouin-Wigner perturbation theory (equivalent to a Schrieffer-Wolff transformation [22]). We thereby eliminate the charge degrees of freedom on the metal-ion sites and incorporate their effect in an effective tunnel coupling between the ligands. An example of a virtual process giving rise to this coupling is shown in Figure 4. In the resulting effective model each metal-ion site is thus either entirely eliminated (Fe^{2+}) or characterized by a pure spin degree of freedom (Co^{2+}). This model contains the low energy properties of the mobile electrons on the $[2 \times 2]$-grid. As a result we are left with the effective Hamiltonian (up to a constant):

$$H_{\mathsf{Fe}}^{\mathsf{eff}} = \sum_{\langle jk \rangle} \sum_{\sigma} T\, a_{j,\sigma}^{\dagger} a_{k,\sigma} + H_{\mathsf{L}} \tag{9}$$

$$\begin{aligned} H_{\mathsf{Co}}^{\mathsf{eff}} &= \sum_{\sigma,i} \sum_{j,k=i,i+1} \big\{ (K + J\sigma\tau_i^z) a_{j,\sigma}^{\dagger} a_{k,\sigma} + J\tau_i^{+\sigma} s_{j,k}^{-\sigma} \\ &+ (K + (J-F)\sigma\tau_i^z) n_{j,\sigma} + (J-F)\tau_i^{+\sigma} s_{j,j}^{-\sigma} \big\} \\ &+ H_{\mathsf{L}} \\ &= \sum_{i} \sum_{j,k=i,i+1} \big\{ (J - F\delta_{j,k}) \boldsymbol{\tau}_i \, \mathbf{s}_{j,k} + \sum_{\sigma} K a_{j,\sigma}^{\dagger} a_{k,\sigma} \big\} \\ &+ H_{\mathsf{L}} \end{aligned} \tag{10}$$

The coupling constants T, K and J are

$$\begin{aligned} T &= \frac{t^2}{2\Delta} \\ K &= \frac{1}{2}\left(\frac{t^2}{\Delta} - \frac{t^2}{U-\Delta}\right) \\ J &= \frac{1}{2}\left(\frac{t^2}{\Delta} + \frac{t^2}{U-\Delta}\right). \end{aligned} \tag{11}$$

For Fe^{2+} the effective Hamiltonian is the extended Hubbard model on four ligand sites with effective hopping matrix element T. In contrast, for Co^{2+} we retain an eight site model: the effective Hamiltonian couples the spin and charge on the four ligands to the spin on the four metal-ions. The first two terms in (10) describe tunneling between ligands with (J) and without spin-flip (K). The next two terms describe fluctuations of the charge and spin on the ligands. The exchange coupling $J > 0$, which is counteracted by the direct ferromagnetic exchange $F > 0$, favors a correlated ground state where the ligand and metal-ion spins are coupled antiferromagnetically. This coupling always dominates over the tunneling amplitude K: $J > |K| \geqslant 0$ and K even vanishes for $\Delta = \frac{U}{2}$. The sign of K depends on whether $\Delta < \frac{U}{2} (K > 0)$ or $\Delta > \frac{U}{2} (K < 0)$ and determines whether the amplitude $K + J$ for the tunneling of electrons with spin σ parallel to the local spin on the metal-ion $\boldsymbol{S}_i$ is enhanced/suppressed relative to the amplitude $K - J$ for spin antiparallel to $\boldsymbol{S}_i$.

We point out that the effective Hamiltonian (10) for Co^{2+} contains no explicit interaction term between the metal-ion spins: all interactions are mediated by the electrons on the ligands. In order to describe the electron addition effects on the metal-ion spin coupling our second-order perturbation theory suffices. In the absence of extra electrons on the ligands, only in fourth-order perturbation theory a weak effective antiferromagnetic Heisenberg exchange interaction between the spins on the metal-ions appears. This superexchange is mediated by an empty intermediate ligand orbital. The four site Heisenberg-model with this effective coupling has been

studied in [14] and agrees with intramolecular coupling found experimentally. As soon as a ligand orbital contains one electron, the weak fourth order effect is superseded by the second order coupling incorporated in the effective Hamiltonian (10).

V. ADDITION ENERGIES AND SPIN STATES

We now present the results for the effective Hamiltonian (9),(10) (perturbation theory) and the full Hamiltonian (1) . We first study the addition energy spectra which reflect mainly the electrostatic effects and then focus on the spin properties of the ground states and lowest lying excited states as a function of the number of *added* electrons n.

A. Fe^{2+}-grid

To highlight the effect of the electrostatic interactions, we first consider the *noninteracting* limit of the effective 4-orbital model (9) for Fe^{2+} ($u, v, w \ll |T|$). Of the four eigenstates the lowest one lies at energy $\epsilon - 2|T|$, two states are orbitally degenerate at ϵ (due to the 4-fold symmetry axis) and the highest state lies at $\epsilon + 2|T|$. Electron addition in this case would give rise to a pair of twofold degenerate peaks with a fourfold degenerate peak in between. This is in clear qualitative disagreement with the experiments [12]. The addition spectrum can only be understood by including the interactions $u > v > w > |T|$ in our effective model (9). The first electron reduces one of the four ligands. The next one goes onto the opposite ligand in order to minimize the Coulomb interaction. The third and fourth electrons reduce the adjacent ligands. For the next four electrons this sequence of processes is repeated, each time doubly occupying a ligand orbital. We thus have two sets of four reduction peaks separated by a large gap of order u. Each set of four consists of two pairs of closely spaced peaks (distance w) separated by a moderate gap $2v - w < u$. The tunneling between equivalent ligands only weakly affects this picture. In Figure 5 we plot the addition energies as a function of the tunneling amplitude t.

Now we discuss the ground state spin as successive electrons are added to the ligands. Filling the levels in the *noninteracting* case of the effective model (9) ($u, v, w \ll |T|$) according to the Pauli principle the ground state spin is $S_{\mathsf{tot}} = 1/2$ for odd particle number n. For even $n = 2, 6$ the ground state spin is $S_{\mathsf{tot}} = 0$, whereas for half-filling ($n = 4$) $S_{\mathsf{tot}} = 0$ and $S_{\mathsf{tot}} = 1$ are degenerate. In the presence of interactions charge fluctuations are suppressed. For $u \gg |T|$ this gives rise at $n = 4$ to a Heisenberg antiferromagnet with a singlet ground state (Figure 6).

For *sufficiently large* $u > u_{\mathsf{th}}^{\mathsf{Fe}}$ (Figure 7) the ground state spin for odd $n = 3, 5$ is enhanced from the noninteracting value $S_{\mathsf{tot}} = 1/2$ to the maximal possible value

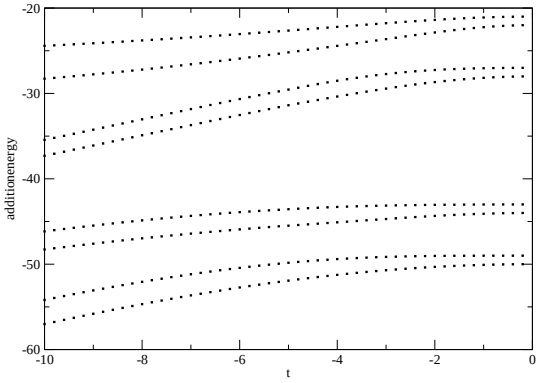

FIG. 5: Addition energy of Fe^{2+}-[2×2]-grid as function of tunneling t (in units of w) for $u = 15, v = 3, w = 1, \Delta = -50, U = 100$ calculated from the full model 1. For $|t| < |\Delta|$ we are in the perturbative regime where no spin is localized on the Fe^{2+} site and the effective model (9) applies. We reproduce the addition energy spectrum measured in [12] where the spacings between the ground state energies with different n are due to electrostatic interactions.

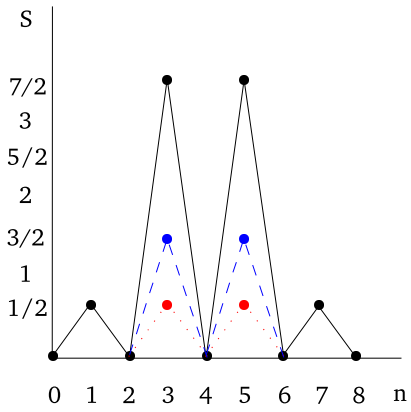

FIG. 6: Ground-state spin as function of the number of electrons n added to the ligands for $u > u_{\mathsf{th}}$ (dashed blue line = Fe^{2+}, black line = Co^{2+} without direct exchange) and for $u < u_{\mathsf{th}}$ (dotted red line in both cases).

$S_{\mathsf{tot}} = 3/2$ (Figure 6). Now the tunneling between the ligands plays a decisive role. Because double occupation is suppressed, a single hole/electron (relative to the half-filled state $n = 4$) can maximally gain kinetic energy when the background of the other electrons is fully spin polarized. This ferromagnetic alignment competes with the antiferromagnetic spin coupling due to superexchange processes. Which process dominates depends on the strength of the onsite repulsion u relative to the hopping $|T|$ i.e. $u_{\mathsf{th}}^{\mathsf{Fe}} \propto |T|$. The gap between maximal spin ground state and lowest excited state saturates at a value

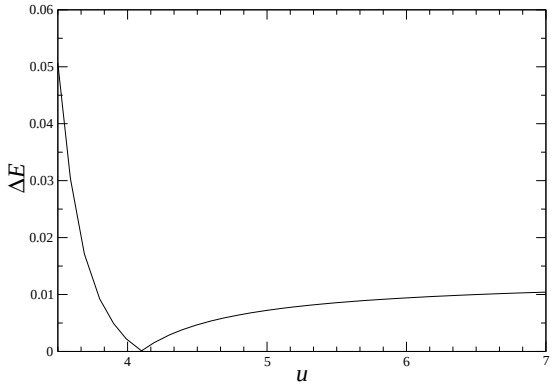

FIG. 7: Fe^{2+}-$[2\times 2]$-grid: Ground-excited state gap as function of u for $n=3$, $\Delta=-10, v=2.25, w=1$. For $u>u_{\mathsf{th}}\approx 4.15$ the ground state has maximal spin.

$\sim 2|T|$ independent of u due to the kinetic origin of the effect. This is the underlying mechanism for the Nagaoka theorem [15] which guarantees that the ground state has maximal spin if u is larger than some positive threshold value. It applies to the effective model (9) because it fulfills a certain connectivity condition for the lattice, namely that a so-called "exchange loop" exists which is no longer than four sites [23, 24]. This implies that all basis states with common S^z_{tot} are connected with each other via nonvanishing matrix elements of (9) [24]. In order to attain an observable effect one should have a moderate T on the one hand, and on the other hand the onsite interaction u must be enhanced with increasing T. The latter can be achieved by a chemical modification of the ligands that draw charge density in the ligand LUMO orbitals. Taking typical parameters [12] $|\Delta|\approx 1eV, t\approx 10^{-1}eV, \Delta E_{\mathsf{Nag}}\approx 10^{-2}eV$, we estimate $u_{\mathsf{th}}\approx 1eV$ which is reasonable.

We have checked that the interactions v, w increase the critical value $u^{\mathsf{Fe}}_{\mathsf{th}}$ for the Nagaoka state but do not destroy it [16]. We have also analyzed the effect of disorder by making the ligand sites inequivalent through different MLCT barriers Δl. As expected, the Nagaoka state is stable if the change in the MLCT barrier Δ is smaller than $|T|$. Otherwise, due to the localization of electrons the Nagaoka effect, which is of kinetic nature, is suppressed. We expect disorder effects to be relatively weak since the ligands and the metal-ions form a highly symmetric grid of equivalent centers.

B. Co^{2+}-grid

The addition energy spectrum which we obtain for the Co^{2+}-grid is qualitatively the same as for the Fe^{2+}-grid since electrostatic interactions dominate. In the experiment [12] the reduction peaks corresponding to the first three electrons are similar to those of Fe^{2+}, in agreement with our model. However, the next five peaks exhibit roughly a constant spacing $\sim 0.25-0.3eV$, corresponding to the charging of one big "island" with better screening. This would require in our model to artificially change the parameters to $u\approx v\approx w\approx 0.3eV$ beyond $n=3$. Obviously effects become important which are not included in our electronic low temperature model, e.g. adding electrons could result in a change in the molecular geometry which will lead to different electrostatic interactions. Also at the high experimental temperatures individual Co^{2+} ions may be in the high-spin state where the π-symmetric t_{2g}-orbitals are singly occupied. These can couple more strongly to the ligand orbitals and increase metal-ligand charge transfer. Here we are interested in the low temperature regime however and assume low-spin ($S=1/2$) Co^{2+} ions.

The spin properties of the eigenstates of the effective model (10) without direct exchange interaction, i.e. $F=0$, are qualitatively similar to Fe^{2+} (Figure 6) and will be considered first. We have a singlet ground state at half-filling ($n=4$), and a Nagaoka maximal-spin ground state near half-filling ($n=3,5$) for sufficiently large charging ($U>u>u^{\mathsf{Co}}_{\mathsf{th}}$). At half-filling $n=4$ the antiferromagnetic Néel-state has the largest weight in the ground state. The electron spins on the metal-ions couple ferromagnetically due to the presence of electrons on the ligands and *and vice versa*. This is to be contrasted to the situation at $n=0$ where the metal-ion spins couple antiferromagnetically and at $n=4$ for the Fe^{2+}-$[2\times 2]$-grid, where the electron spins on adjacent ligands couple antiferromagnetically. The total spins of the metal-ion and ligand sublattice couple antiferromagnetically to a singlet ground state. The appearance of the Nagaoka state at $n=3,5$ has a different origin than in the Fe^{2+}-$[2\times 2]$-grid since we have exchange loops longer than four sites. We do, however, have a bipartite lattice and hopping occurs only between the ligand and metal-ion sublattices. This is also a sufficient condition for the Nagaoka theorem to apply [16, 24].

The four spins on the bridging Co^{2+} metal-ions cause two quantitative differences from the case of Fe^{2+}. Firstly, the maximal spin value attained in the Nagaoka state is simply larger, $S_{\mathsf{tot}}=7/2$. Secondly, the threshold value of $u^{\mathsf{Co}}_{\mathsf{th}}$ for the appearance of this state is dramatically increased, $u^{\mathsf{Co}}_{\mathsf{th}}\approx 10^4$ in both the full and effective models. This is due to the antiferromagnetic exchange coupling J between the metal-ion and ligand sublattices. This suppression of ferromagnetism can however be understood by considering two extreme limits. In the limit where two sublattices are equivalent ($\Delta=0, u=U$) Nagaoka's mechanism is ineffective because the exchange paths are to long (>4 sites, [24]). This implies that with decreasing Δ a higher $u^{\mathsf{Co}}_{\mathsf{th}}$ is required to stabilize the Nagaoka state. In the opposite limit where the sublattices are well separated in energy ($\Delta, U-\Delta\gg|t|$), the effective model (10) applies and $u^{\mathsf{Co}}_{\mathsf{th}}$ is decreased. The maximal spin state can still be achieved when U is sufficiently increased for *fixed* Δ, such that $t\ll\Delta\ll U/2$ we have $K\approx -J$: tunneling of electrons with spins antiparallel to the metal spins is

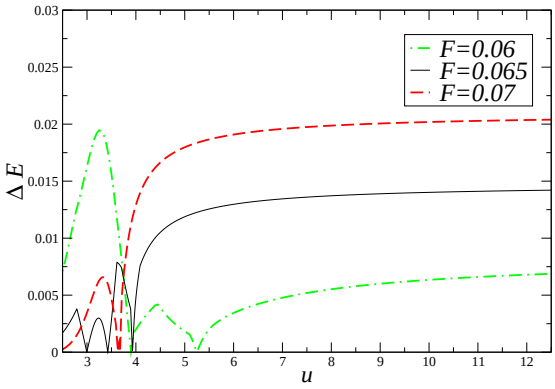

FIG. 8: Co^{2+}-$[2 \times 2]$-grid: Ground-excited state gap as function of u for $n = 3$, $\Delta = 10, U = 100, v = 2.25, w = 1$ and three different values for the direct exchange $F = 0.06, 0.065, 0.07$. The non-monotonic behavior of the gap is due to several level crossings until the Nagaoka state is the ground state (beyond the rightmost zero). The direct exchange "kicks" the system into the Nagaoka state: the threshold value $u_{\mathsf{th}}^{\mathsf{Co}}$ is reduced when $F \to J = 0.06$. Even for smaller $F > 0$ one still needs $u > u_{\mathsf{th}}^{\mathsf{Co}}$ to drive the system into the maximal spin ground state.

suppressed, favoring a polarized ground state. However, the splitting ΔE is decreased due to the small effective coupling constants.

The neglect of any (even small) direct exchange represents an unbalanced treatment of the magnetic coupling, since the Nagaoka mechanism and the direct exchange are known to cooperate to stabilize maximal spin states [16]. Even when it is weak, $F \approx J$, the direct exchange leads to a dramatic reduction of the threshold Coulomb energy for achieving the Nagaoka state to values more close to those found above for Fe^{2+}: $u_{\mathsf{th}}^{\mathsf{Co}} \sim 5$ (Figure 8) and the gap between ground and excited state increases again. Furthermore it is possible that an enhanced direct exchange stabilizes a maximal spin state even at half-filling $n = 4$. Still the spin can be switched from 0 to 7/2 by going from $n = 2$ to $n = 3$ (or from $n = 5$ to $n = 6$). The excitation gap ΔE as function of u (Fig. 8) saturates at values of the order of $0.2J$. In this limit the direct exchange "kicks" [16] the system into the Nagaoka state. For $F \gg J$ the ferromagnetic coupling exceeds the exchange coupling and the resulting ground state is always ferromagnetic, independent of u indicating the Nagaoka mechanism is not relevant anymore.

VI. CONCLUSION

We have analyzed a strongly-correlated electron model for a $[2 \times 2]$-grid complex with four transition-metal centers (either Fe^{2+} or Co^{2+}) to illustrate the interplay between electron addition and intramolecular spin coupling. Our model contains both localized magnetic moments and delocalized electrons, in contrast to the customary description of molecular magnets. We have based our model on the addition energy spectra of the experiments in Ref.[12], the crucial input being that the extra electrons occupy ligand orbitals. We found large changes in the total spin, $\Delta S_{\mathsf{tot}} > 1/2$, of the molecule upon variation of the total electron number due to the Nagaoka mechanism. The large charging energies on the ligands required for the high spin states can be tuned chemically by adding electron-donating groups to the ligands. Localized spins on the mediating metal ions (Co^{2+}) counteract the Nagaoka effect, but the direct exchange coupling with the neighboring ligands can compensate for this. The total spin in the Nagaoka state for the Co^{2+} complex is therefore more than twice as large as for the Fe^{2+} complex. Low temperature electron tunneling experiments can access the change of the molecular spin as a function of added charge. Spin-blockade effects [18] will dominate the single-electron tunneling around transitions between charge states with maximal spin [19]. Also, the $S_{\mathsf{tot}} = 1/2$ Kondo effect usually expected for odd $n = 3, 5$ will also be suppressed. In any case the Nagaoka mechanism lowers maximal spin states in energy. Even as low lying total-spin excitations Nagaoka states have clear transport fingerprints due to spin-selection rules [19]. Other molecular complexes can also show the above behavior. It is essential that the connectivity of the electron-accepting centers is appropriate [16, 24] for the Nagaoka mechanism to be effective.

Acknowledgments

J. Kortus is acknowledged for stimulating discussions. We thank J.-M. Lehn for providing us experimental data and for discussions. M. R. Wegewijs acknowledges the financial support provided through the European Community's Research Training Networks Program under contract HPRN-CT-2002-00302, Spintronics.

[1] R. Sessoli, H. L. Tsai, A. R. Schake, S. Wang, J. B. Vincent, K. Folting, D. Gatteschi, G. Christou, and D. N. Hendrickson, JACS **115**, 1804 (1993).
[2] S. M. J. Aubin, Z. Sun, L. Pardi, J. Krzystek, K. Folting, L. C. Brunel, A. L. Rheingold, G. Cristou, and D. N. Hendrickson, Inorg. Chem. **38**, 5329 (1999).
[3] J. R. Friedman, M. P. Sarachick, J. Tejada, and R. Ziolo, Phys. Rev. Lett. **76**, 3830 (1996).
[4] W. Wernsdorfer and R. Sessoli, Science **284**, 133 (1999).
[5] A. Chiolero and D. Loss, Phys. Rev. Lett. **80**, 169 (1998).
[6] F. Meier and D. Loss, Phys. Rev. Lett. **86**, 5373 (2001).
[7] O. Waldmann, T. Guidi, S. Carretta, C. Mondelli, and A. L. Dearden, Phys. Rev. Lett. **91**, 237202 (2003).
[8] L. Zhao, C. Matthews, L. Thomson, and S. Heath, Chem.

Commun. **4**, 265 (2000).
[9] M. Ruben, J. Rojo, F. Romero-Salguero, L. Uppadine, and J.-M. Lehn, Angew. Chem. Int. Ed. **43**, 3644 (2004).
[10] J.-M. Lehn, *Supramolecular chemistry: Concepts and perspectives* (VCH, Weinheim, 1995).
[11] G. Hanan, D. V. U. Schubert, J.-M. Lehn, G. Baum, and D. Fenske, Angew. Chemie Int. Ed. **36**, 1842 (1997).
[12] M. Ruben, E. Breuning, M. Barboui, J.-M. Gisselbrecht, and J.-M. Lehn, Chem. Eur. J. **9**, 291 (2003).
[13] A. Semenow, J. Spatz, M. Möller, J.-M. Lehn, B. Sell, D. Schubert, C. Weidl, and U. Schubert, Angew. Chemie Int. Ed. **38**, 2547 (1999).
[14] O. Waldmann, J. Hassmann, P. Müller, G. S. Hanan, D. Volkmer, U. S. Schubert, and J.-M. Lehn, Phys. Rev. Lett. **78**, 3390 (1997).
[15] Y. Nagaoka, Phys. Rev. **147**, 392 (1966).
[16] M. Kollar, R. Strack, and D. Vollhardt, Phys. Rev. B **53**, 9225 (1996).
[17] P. Gütlich, A. Hauser, and H. Spiering, Angew. Chemie Int. Ed. **33**, 2024 (1994).
[18] D. Weinmann, W. Häusler, and B. Kramer, Phys. Rev. Lett. **74**, 984 (1995).
[19] C. Romeike, M. R. Wegewijs, and H. Schoeller, submitted to Phys. Rev. B.
[20] K. Ono and S. Tarucha, cond-mat/0309062 (2003).
[21] A. A. Vlček, Coord. Chem. Rev. **43**, 39 (1982).
[22] J. Schrieffer and P. Wolff, Phys. Rev. **149**, 491 (1966).
[23] H. Tasaki, Phys. Rev. B **40**, 9192 (1989).
[24] H. Tasaki, Progress of Theoretical Physics **99**, 489 (1998).